Available online at www.sciencedirect.com
ScienceDirect
Trans. Nonferrous Met. Soc. China 33(2023) 917−928
Transactions of Nonferrous Metals Society of China
www.tnmsc.cn

Release mechanism of impurity potassium in molybdenum concentrate treatment process

Qi-hang LIU[1,2], Qu HU[1], Di WANG[1], Shuang-ping YANG[1], Kai HE[2]

1. School of Metallurgical Engineering, Xi'an University of Architecture and Technology, Xi'an 710055, China;
2. Technical Centre, Jinduicheng Molybdenum Co., Ltd., Xi'an 710077, China

Received 3 November 2021; accepted 8 July 2022

Abstract: The kinetic characteristics and mechanism of potassium release in the molybdenum concentrate treatment process were studied by kinetic analysis and analytical techniques such as SEM−EDS, MLA and ICP. The results show that the first-order kinetic model is the best kinetic model of potassium release in the water washing and ammonia leaching process. Potassium is present in molybdenum concentrate in the form of soluble potassium ions and four potassium minerals. During the roasting process of molybdenum concentrate, some muscovite decomposed into orthoclase, while other muscovite combined with impurity metal elements to form anandite. Furthermore, the transformation of muscovite to orthoclase could be effectively inhibited by the rapid cooling of molybdenum calcine. The results could provide a basis for reducing potassium content in ammonium molybdate products.
Key words: molybdenum concentrate; potassium removal; roasting; potassium minerals; ammonium molybdate

1 Introduction

High purity molybdenum and its compounds are widely used in metallurgy, electronic information, medical and other fields [1,2]. Potassium has an adverse effect on molybdenum products such as refractory materials and electronic components. For example, molybdenum is usually used as a material for electric light sources, and the impurity potassium in it is easily volatilized at high temperatures. After the volatilized potassium is combined with the heating element or light source device, the insulating properties of components would be affected by potassium impurities in the form of strong alkalis [3−5]. Therefore, reducing the potassium content in molybdenum products is a key measure to prolong the service life of industrial devices [5,6].

The raw material used to produce high purity molybdenum and its compounds is molybdenum concentrate [7,8]. One of the most effective measures to produce low potassium molybdenum products is the removal of potassium in the treatment process of molybdenum concentrate [9−11]. In the production process of roasting−washing−ammonia leaching of the molybdenum concentrate, the total content of potassium generally decreases due to the removal of soluble potassium ions during the water washing process [12,13]. However, insoluble potassium minerals are not easily removed by water washing, and they would release part of potassium into ammonia leaching solution (ammonium molybdate) in the process of ammonia leaching [14,15]. The results show that the K/Mo of molybdenum concentrate is generally 5000−7000 mg/kg, and the K/Mo of ammonium molybdate is 100−300 mg/kg [16]. The potassium in ammonium molybdate is mostly derived from potassium minerals which are insoluble in water.

Corresponding author: Qi-hang LIU, Tel: +86-17792324750, E-mail: liuqh@xauat.edu.cn
DOI: 10.1016/S1003-6326(23)66155-2

In recent years, acid leaching, which could effectively remove the mineral potassium, have been completely prohibited due to the environmental protection. Consequently, water washing have become the main method of potassium removal [16−18]. It is necessary to study the release kinetics of potassium during water washing and subsequent ammonia leaching [19,20]. In addition, quantitative analysis of potassium forms during water washing and ammonia leaching helps to clarify the release mechanism of potassium and provide a theoretical support for further potassium removal [21]. However, the absolute content of potassium minerals in ammonia molybdate production process is generally in the order of 10^{-3}−10^{-5}. Thus, it is difficult to study the potassium release mechanism of various minerals by traditional analysis methods such as XRD and SEM−EDS [22−24].

Mineral liberation analyzer (MLA) technology which contains a high-speed automatic mineral parameter quantitative analysis system, was launched in April 2013 [25,26]. At present, MLA is mainly used in geoscience, mining and other fields, and there is no report on the application of MLA technology to the analysis of potassium minerals in the production process of ammonium molybdate [26,27]. This work studied the kinetic characteristics of potassium release in the treatment process of molybdenum concentrate. Furthermore, the potassium release mechanism of different potassium minerals was revealed by MLA, SEM−EDS, etc.

2 Experimental

2.1 Treatment of molybdenum concentrate

The samples of molybdenum concentrate used in the experiment were taken from a molybdenum production enterprise in China. The main chemical composition of molybdenum concentrate is shown in Table 1. Firstly, 100 g samples of molybdenum concentrate were taken each time and placed in a flat long crucible. Then the samples were roasted in a high-temperature box resistance furnace to simulate the actual production conditions. The roasting temperature was 300−600 °C. After being roasted for different time, the samples were cooled by rapid cooling and slow cooling, respectively.

The rapid cooling adopted 0 °C ice water for direct cooling, and the solid−liquid mass ratio was set to 1:5. After that, the cooled samples were taken out and immersed in 1 L of deionized water, stirred for 5 min, and then left to stand for different times. Each sample was washed three times with water, and all washed samples were dried in an electric oven at a constant temperature. Finally, the samples were ground by an omnidirectional planetary ball mill (DQM−4L), and then soaked in ammonia water with a concentration of 25%.

Table 1 Main chemical composition of molybdenum concentrate (wt.%)

Total K	Mineral K	Mo	S	Si
0.21	0.13	57.1	22.3	0.87

Fe	Al	Ca	Na	Cu	Mg
0.79	0.26	0.33	0.3	0.04	0.04

2.2 Determination of potassium in different samples

(1) The samples of raw molybdenum concentrate, molybdenum calcine after roasting at 580 °C for 6 h, molybdenum calcine after water washing (water washing residue) and ammonia leaching residue were prepared. The type and content of minerals in these samples were analyzed by X-ray fluorescence spectrometry (ZSX100e), SEM−EDS (JSM−5610V) and MLA. The MLA used in this experiment was composed of SEM (Sigma 300), Bruker energy spectrometer (Quantax 400), and Bruker AMICS (Advanced Mineral Identification and Characterization System) mineral analysis software. The test temperature was 24 °C, the voltage was 20 kV, and the scanning accuracy was 1.12 μm. Each specimen was formed into a sheet (48 mm × 26 mm) and tested after polishing.

(2) In the water washing process of molybdenum calcine, the samples of 10 mL aqueous solution were collected at 15 min intervals, and all liquid samples were filtered with filter papers for 3−5 times. Afterwards, the prepared samples were taken out for potassium content determination by inductively coupled plasma spectrometry (ICP−OES: Aglient 5110). Similarly, the samples of 10 mL ammonia leaching solution were collected every 15 min during the ammonia leaching process, and the liquid samples were also filtered with filter papers 3−5 times. Then all the prepared samples of ammonia leaching solution were taken out for potassium content determination by ICP−OES.

3 Results and discussion

3.1 Kinetic analysis of potassium release

During water washing and ammonia leaching of molybdenum calcine, the concentration of potassium in aqueous solution and ammonia leaching solution was obtained by the method in Section 2.2, and the cumulative release of potassium was calculated by

$$S=CV/m \quad (1)$$

where S is the release amount of potassium in aqueous solution or ammonia leaching solution, mg·kg^{-1}; C is the concentration of potassium in the collection solution, mg·L^{-1}; V is the volume of the collection solution, L; m is the mass of the molybdenum calcine sample used in each experiment, kg.

The cumulative release amount of potassium of molybdenum calcine during water washing and ammonia leaching was obtained from Eq. (1), as shown in Fig. 1.

As shown in Fig. 1, the concentration of potassium in the solution gradually increases with the increase of water washing and ammonia leaching time. The results indicate that potassium in molybdenum calcine can be partially removed by water washing. However, the potassium content of ammonium molybdate products increased with the ammonia leaching time prolonged, which is not conducive to the production of low potassium products. Compared with the ammonia leaching process, the potassium concentration increased rapidly in the early stage of water washing, and increased slowly in the later stage. This may be due to the rapid release of water-soluble potassium in the early stage and the slower release of potassium from potassium minerals in the later stage.

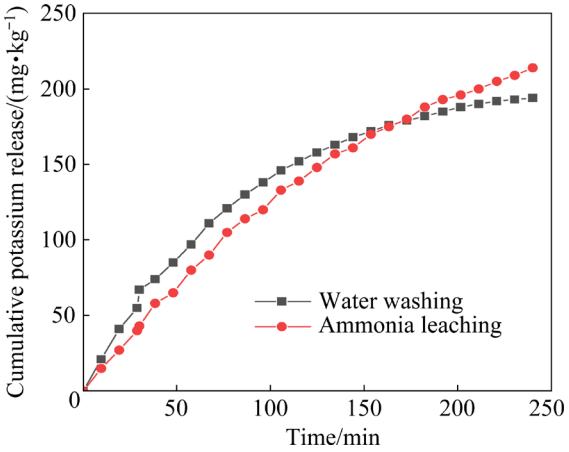

Fig. 1 Cumulative release of potassium during water washing and ammonia leaching

3.1.1 Fitting results

Based on the mentioned characteristics, the potassium release kinetic process of water washing was simulated in stages. The parabolic diffusion model, double constant model, Elovich model and first-order kinetic model were used to simulate the potassium release process of water washing and ammonia leaching respectively. The kinetic equations of different models are as follows:

(1) Parabolic diffusion model: $y=a+bx^{0.5}$;

(2) Double constant model: $y=ax^{b}$;

(3) Elovich model: $y=a+b\ln x$;

(4) First-order kinetic model: $y=a[1-\exp(-bx)]$

where y is the cumulative release of potassium at time x, x is the reaction time, and a and b are the model parameters. The superior fit of the model refers to the load degree between the expected value and the measured value of the model. The correlation coefficient R^2 and regression standard deviation (SD) are usually used to judge. The larger the value of R^2, the smaller the value of SD, indicating the better fitting of the model.

The staged kinetic simulation of water washing and the overall kinetic simulation of ammonia leaching were carried out respectively. The fitting results are shown in Table 2 and Table 3.

During the water washing and ammonia leaching process, the fitting equations of different kinetic models were obtained as shown in Table 2.

Table 2 Fitting equations for different kinetic models

Treatment method	Time/min	Parabolic diffusion model	Double constant model	Elovich model	First-order kinetic model
Water washing	0−105	$y=-17.8+15.44x^{0.5}$	$y=32.9x^{0.71}$	$y=-203+791\ln x$	$y=208[1-\exp(-0.011x)]$
	105−240	$y=60.72+8.85x^{0.5}$	$y=5.27x^{0.3}$	$y=-121+58\ln x$	$y=38[1-\exp(-0.0011x)]$
Ammonia leaching	0−240	$y=-35+16.16x^{0.5}$	$y=4.61x^{0.71}$	$y=-194.6+72\ln x$	$y=290.83[1-\exp(-0.005x)]$

Table 3 Fitting parameters of R^2 and SD for different kinetic models

Treatment method	Time/min	Parabolic diffusion model		Double constant model		Elovich model		First-order kinetic model	
		R^2	SD	R^2	SD	R^2	SD	R^2	SD
Water washing	0−105	0.972	8.0	0.992	3.59	0.924	11	0.999	2.56
	105−240	0.977	2.17	0.980	1.93	0.989	1.47	0.999	0.39
Ammonia leaching	0−240	0.983	8.96	0.980	6.28	0.948	14.27	0.999	2.1

As can be seen from Table 3, the fitting degree of potassium release kinetic model of molybdenum calcine under water washing is as follows. Early stage (0−150 min): first-order kinetic model > double constant model > parabolic diffusion model > Elovich model; Later stage (150−240 min): first-order kinetic model > Elovich model > double constant model > parabolic diffusion model. The fitting degree of potassium release kinetic model of washed molybdenum calcine under ammonia leaching is as follows: first-order kinetic model > parabolic diffusion model > double constant model > Elovich model.

The fitting results of water washing and ammonia leaching processes simulated by the first-order kinetic model are shown in Fig. 2.

It can be seen that when the first-order kinetic model was used for fitting, the correlation coefficient was more than 0.995. The standard deviation between the simulated value and the real value of the cumulative release of potassium under ammonia leaching and water washing was 0.39−2.56.

3.1.2 Kinetic parameter analysis of potassium release

According to the fitting results of the kinetic model in Section 3.1.1, the values of the parameters a and b of different kinetic models were obtained, as shown in Table 4.

For the double constant equation, the initial instantaneous rate of the potassium release process is represented by the value of a. The larger the value of a, the greater the initial instantaneous release rate of potassium. By comparing a of the double constant equation, it can be seen that the initial instantaneous release rate of potassium in the early stage of water washing is greater than that in the later stage of water washing and ammonia leaching. This indicates that water-soluble potassium can be quickly dissolved in water and removed in the early stage of water washing.

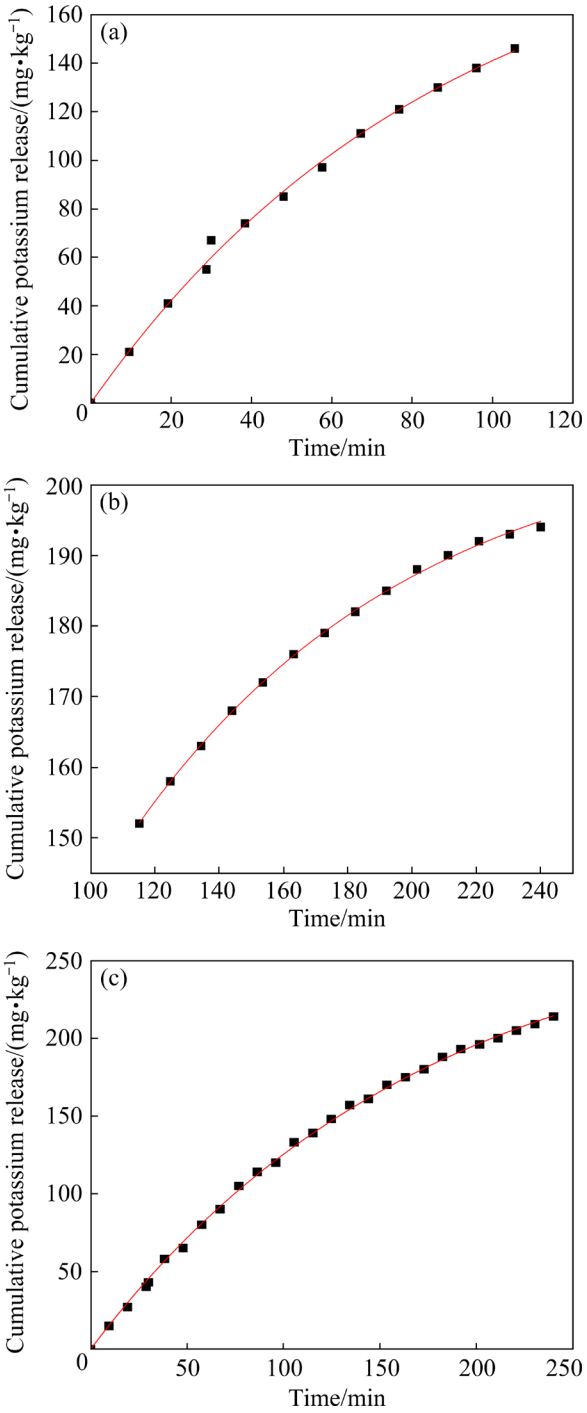

Fig. 2 Fitting results of first-order kinetic model: (a) In early stage of water washing; (b) In later stage of water washing; (c) Ammonia leaching

Table 4 Different kinetic model parameters

Treatment method	Time/ min	Double constant model		Elovich model		First-order kinetic model	
		a	*b*	*a*	*b*	*a*	*b*
Water washing	0−105	32.9	0.71	−203	791	208	0.011
	105−240	5.27	0.3	−121	58	38	0.011
Ammonia leaching	0−240	4.61	0.71	−194.6	72	290.83	0.005

The Elovich rate equation was obtained by taking the derivative of Elovich equation, $y=b/x$. The release rate at any time x is represented by the value of b, the larger the value of b, the greater the release rate of potassium. It can be seen from Table 4 that in the washing process, the average potassium release rate within 0−150 min in the early stage is significantly greater than that within 150−240 min in the later stage. In addition, compared with the release rate of mineral potassium in the later stage of washing, the average release rate of potassium in the ammonia leaching process is greater. It suggests that the mineral potassium is more likely to release potassium into the ammonia leaching solution in the ammonia leaching process.

The maximum equilibrium release during the release process is represented by a of the first-order kinetic equation. It can be seen from Table 4 that the a of the first-order kinetic equation of ammonia leaching is significantly larger than that of water washing. It illustrates that the maximum equilibrium release of potassium during ammonia leaching is greater than that of water washing, negatively affecting ammonium molybdate products' quality.

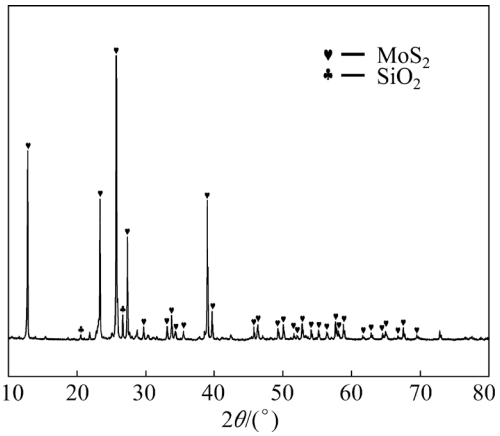

Fig. 3 XRD pattern of molybdenum concentrate

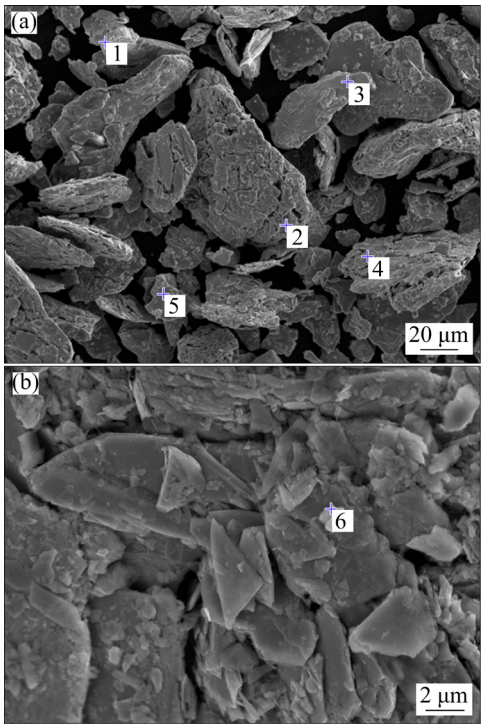

Fig. 4 SEM−EDS analysis of molybdenum concentrate: (a) Electronic image 1; (b) Electronic image 2

3.2 Release mechanism of mineral potassium

3.2.1 Transformation of potassium minerals during treatment

As shown in Fig. 3, Fig. 4 and Table 5, XRD and SEM−EDS were used to analyze molybdenum concentrate used in the experiment, in order to further explore the transformation of potassium in the production process of ammonium molybdate.

As shown in Fig. 3, MoS_2 is the primary component of molybdenum concentrate, with a content of about 95%. The diffraction peak of other impurities is not visible due to the low content, leaving only SiO_2. However, as the SEM−EDS data demonstrated in Fig. 4, the potassium minerals in molybdenum concentrate are orthoclase, muscovite, illite and anandite. Graph 3 illustrates that molybdenum in molybdenum concentrate is present as molybdenum sulfide. A preliminary understanding of potassium minerals in molybdenum concentrates can be obtained by X-ray diffraction

analysis. However, since these potassium minerals with such low content could not be reliably quantified, modern MLA technology was employed to scan and quantify trace minerals in this study. The type and absolute content of minerals in molybdenum concentrate, roasted molybdenum calcine, molybdenum calcine after washing and ammonia leaching residue were determined by MLA. The mineral composition of the molybdenum concentrate used in the experiment is shown in Table 6.

The total potassium content of molybdenum concentrate, molybdenum calcine (roasting at 580 °C for 6 h), washed molybdenum calcine and ammonia leaching residue were determined as shown in Table 7.

As shown in Table 7, the potassium content in the raw molybdenum concentrate is 0.21%, and the

Table 5 Chemical composition of each point in Fig. 4 (wt.%)

Point No.	O	Mg	Al	Si	S	K	Fe	Mo	Mineral
1	41.93	0.88	15.61	25.95		10.33	5.31		Anandite
2	39.47		10.16	35.02		15.35			Orthoclase
3					42.27			57.73	Molybdenite
4	46.10			53.90					Quartz
5	43.21	0.48	19.06	27.99		9.26			Muscovite
6	28.29		17.98	39.9		13.8	28.29		Illite

Table 6 Analysis results of molybdenum concentrate by MLA

Name	Chemical formula	Mass fraction/%	Area fraction/%	Area/ μm^2	Particle number
Native iron	Fe	0.02	0.01	479.27	1
Rutile	TiO_2	0.01	0.01	260.85	3
Calcite	$CaCO_3$	0.01	0.01	419.36	9
Chlorite	$Fe_2 3Mg_{1.5}AlFe_3 0.5Si_3AlO_{12}(OH)_6$	0.02	0.04	1092.09	16
Hematite	Fe_2O_3	0.04	0.03	999.73	18
Kaolinite	$Al_2Si_2O_5(OH)_4$	0.04	0.06	1699.92	16
Illite	$K_{0.6}(H_3O)_{0.4}Al1.3Mg_{0.3}Fe_2 0.1Si_{3.5}O_{10}(OH)$	0.02	0.04	1102.08	18
Fluorite	CaF_2	0.08	0.13	3774.28	19
Orthoclase	$KAlSi_3O_8$	0.04	0.07	2045.65	20
Chalcopyrite	$CuFeS_2$	0.04	0.04	1253.1	20
Anandite	$Ba_{0.75}K_{0.25}Fe_2 2.25Mg_{0.75}Si_3Al_{0.7}Fe_3 0.3O_{10}S_{1.5}(OH)_{0.5}$	0.04	0.04	1190.69	26
Miniumite	Pb_2PbO4	0.11	0.07	2020.69	58
Muscovite	$KAl_3Si_3O_{10}(OH)_{1.8}F_{0.2}$	0.36	0.63	18799	102
Quartz	SiO_2	0.27	0.51	15371.7	93
Anhydrite	$CaSO_4$	0.15	0.25	7366.33	144
Pyrite	FeS_2	1.23	0.21	36359.88	297
Hole		0	6.4	190931.8	23350
Molybdenite	MoS_2	95.57	85.61	2554936	25206
Unknown mineral			4.81	143533.6	15992

Table 7 Potassium content of different samples (wt.%)

Molybdenum concentrate	Molybdenum calcine	Washed molybdenum calcine	Ammonia leaching residue
0.21	0.23	0.12	0.53

potassium content slightly increases after roasting at a high temperature. This is mainly due to the decrease in the total mass of the molybdenum concentrate after being oxidized. The soluble potassium in molybdenum concentrate is mostly removed after the molybdenum calcine is washed. In the process of ammonia leaching, most of potassium minerals remain in the ammonia leaching residue. Potassium is released into the ammonia leaching solution by a small part of the potassium minerals, thus endangering the product quality.

MLA was then used to analyze molybdenum calcine, washed molybdenum calcine and ammonia leaching residue respectively. The particle measurement classification images of different samples are shown in Fig. 5.

As shown in Figs. 5(a) and (b), MoS_2, the main component of molybdenum concentrate, is oxidized to MoO_3. During this process, the content and distribution location of different potassium minerals also changed significantly. The MLA scan images of molybdenum calcine before and after washing are shown in Figs. 5(c) and (d), respectively. It follows that the washing process has little effect on the mineral structure of molybdenum calcine. However, after the washed molybdenum calcine was leached by ammonia, MoO_3, its main component, reacted with ammonia to form ammonium molybdate and entered the solution. As shown in Fig. 5(d), the main component of ammonia leaching residue is quartz (yellow). Compared with molybdenum calcine, the mineral phase structure of ammonia leaching residue changed greatly.

According to the results of the MLA quantitative analysis, the content of potassium minerals in different solid products produced during the treatment was plotted, as shown in Fig. 6 (Sample 1 refers to molybdenum concentrate; Sample 2 refers to molybdenum calcine; Sample 3 refers to washed molybdenum calcine).

As shown in Fig. 6(a), the total content of potassium minerals increases from 0.46% to 1.13% after roasting, and slightly decreases after washing. Combined with the results in Fig. 6(b), it can be inferred that Orthoclase and Muscovite will combine

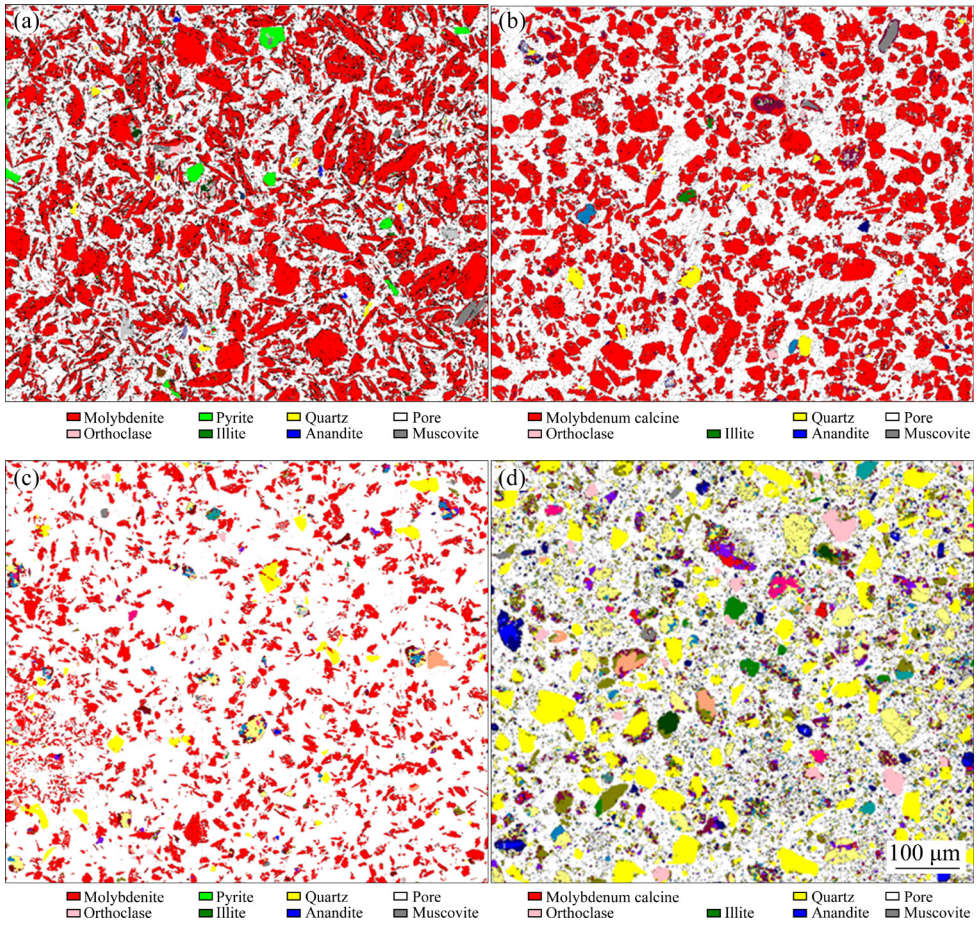

Fig. 5 MLA scan classification images of different samples: (a) Molybdenum concentrate; (b) Molybdenum calcine; (c) Washed molybdenum calcine; (d) Ammonia leaching residue

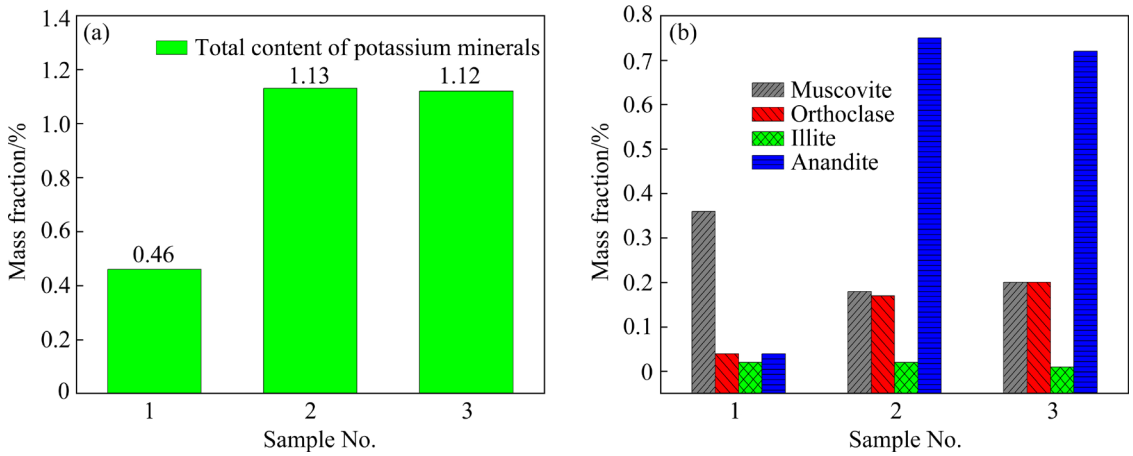

Fig. 6 Variation of potassium minerals in ammonium molybdate production: (a) Total content of potassium minerals; (b) Content of four different potassium minerals

with a large number of impurity metal elements such as Ba, Mg and Fe to form anandite during the roasting process. Furthermore, as shown in Fig. 6(b), the high temperature roasting reduces the muscovite content from 0.36% to 0.07%. The orthoclase content increases from 0.04% to 0.17%, and the anandite content increased from 0.04% to 0.75%. Combined with the chemical formula in Table 6, it can be inferred that high temperature roasting made a considerable part of muscovite decompose into orthoclase. Another part of muscovite reacted with impurity metal elements to generate anandite with large relative molecular weight. The theoretical chemical equation for the decomposition of muscovite into orthoclase was given by the thermodynamic software Factsage as

$$5KAl_2(AlSi_3O_{10})(OH)_{1.8}F_{0.2}= 5KAlSi_3O_8+4H_2O+5Al_2O_3+HF \quad (2)$$

($\Delta G^{\ominus}=94500-130T$)

When the standard Gibbs free energy is 0, the temperature T is 727 K, indicating that the decomposition of muscovite begins at 454 °C.

On the basis of the MLA analysis results, the proportion of potassium minerals in four different samples of molybdenum concentrate, molybdenum calcine, washed molybdenum calcine and ammonia leaching residue are plotted in Fig. 7.

As shown in Figs. 7(a) and (b), after the molybdenum concentrate is roasted at high temperature, the proportion of muscovite decreases from 78.3% to 16.1%. In addition, the proportion of orthoclase and anandite increases from 8.7%, 8.7% to 15.2%, 67% respectively, and illite decreases from 4.3% to 1.8%. It indicates that there is an obvious transformation among potassium minerals during the roasting process of molybdenum concentrate.

As shown in Figs. 7(b) and (c), the proportion of illite and anandite decreases after the molybdenum calcine is washed. Illite and anandite might release part of soluble potassium during the washing process, which is beneficial to the removal of potassium by washing. However, the proportion of muscovite and orthoclase increases, indicating that muscovite and orthoclase might be less prone to release soluble potassium than illite and anandite in the washing process. According to the proportion changes of different potassium minerals before and after the water washing process, the amount of releasing potassium into the aqueous solution in the process of water washing is: illite > anandite > muscovite > orthoclase.

As shown in Figs. 7(c) and (d), the proportion of Anandite and Illite in the ammonia leaching process increases from 63.7%, 0.88% to 76.6%, 5.5% respectively. It illustrates that these two potassium minerals are less likely to enter the ammonia leaching solution (ammonium molybdate) in the ammonia leaching process. However, the proportion of orthoclase and muscovite in the ammonia leaching process decreases from 17.7%, 17.7% to 7.14%, 10.8%. Thus, the amount of potassium released by different minerals into the ammonium molybdate solution during the ammonia leaching process is: orthoclase > muscovite > anandite > illite.

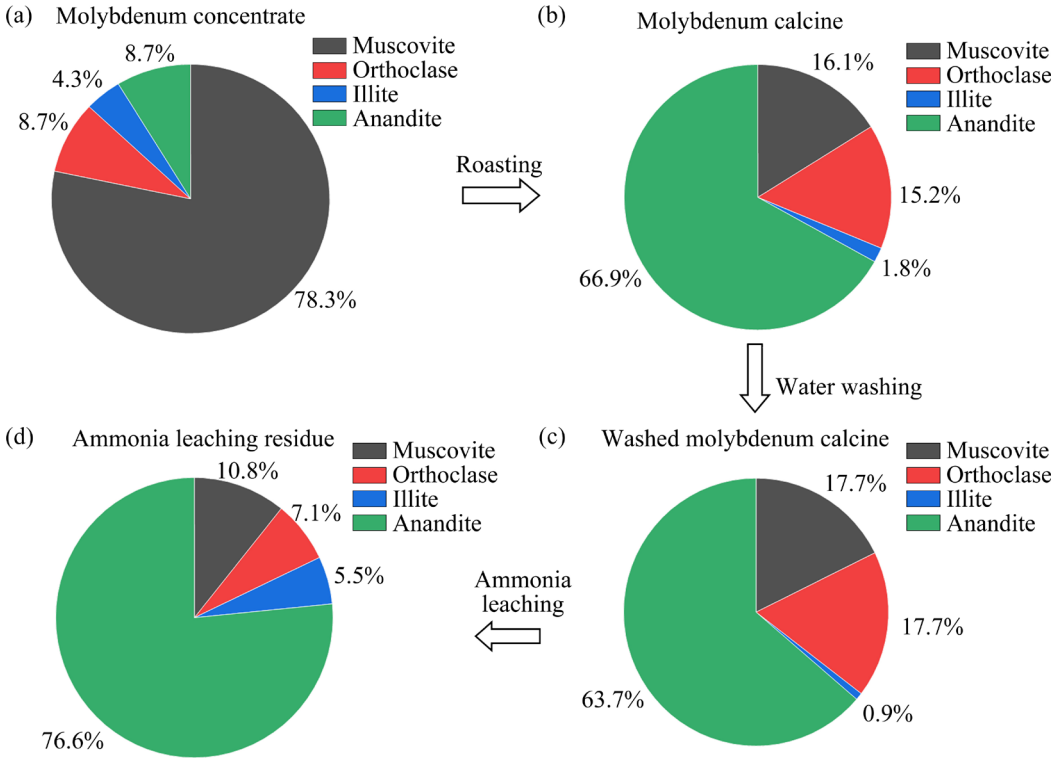

Fig. 7 Proportion change of potassium minerals in ammonium molybdate production process

In summary, compared to the other potassium minerals, the potassium in Orthoclase releases more slowly during the water washing process, but it is the easiest to be released into ammonia leaching solution. Therefore, a high proportion of orthoclase is not conducive to potassium removal.

3.2.2 Effect of cooling method on potassium removal

In order to further verify the analysis results and speculations in Section 3.2.1 and provide guidance for potassium reduction in production, the experimental methods in Sections 2.1 and 2.2 were used to roast molybdenum concentrate at different temperatures for 6 h respectively. Then the molybdenum calcine samples after each roasting were cooled by slow cooling and rapid cooling. After cooling, the samples were taken out for washing and ammonia leaching experiment step by step. The potassium in different solid and liquid products produced during the experiment was detected and analyzed.

Figure 8(a) shows the amount of potassium released from molybdenum calcine roasted at different temperatures for 6 h during ammonia leaching (ammonia leaching time is 3 h). Figure 8(b) shows the amount of potassium released from molybdenum calcine roasted at 550 °C for 6 h under different ammonia leaching time.

In Fig. 8(a), the release amount of potassium in ammonia leaching solution increased with the increase of roasting temperature ranging from 450 to 600 °C. This is because the higher the roasting temperature is, the easier it is for muscovite to decompose into orthoclase. The solubility of orthoclase in ammonia leaching solution is the largest, which leads to the increase of potassium content in ammonium molybdate products. As shown in Fig. 8(b), the release amount of potassium in the ammonia leaching solution also increases gradually with the increase of the ammonia leaching time. In addition, Figs. 8(a) and (b) display that the rapid cooling of molybdenum calcine has an obvious effect on reducing the potassium content in ammonia leaching solution.

In order to further analyze the reasons for the decrease of potassium content in ammonia leaching solution caused by rapid cooling, MLA was used to quantitatively analyze the potassium minerals of molybdenum calcine (roasted at 550 °C for 6 h and then washed with water) under two different cooling methods. The results are shown as Fig. 9 and Table 8.

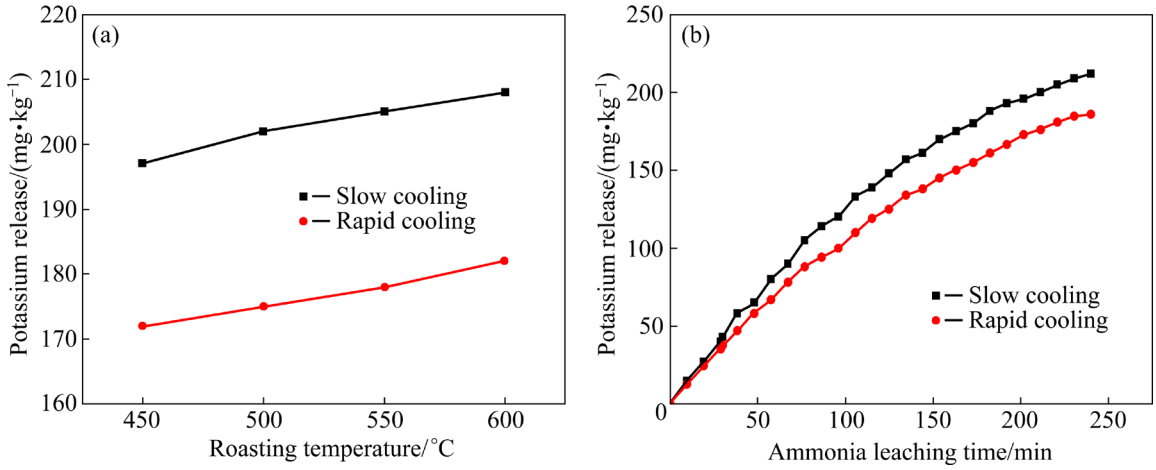

Fig. 8 Effects of cooling methods on potassium content in ammonium molybdate: (a) Potassium release at different roasting temperatures; (b) Potassium release under different ammonia leaching time

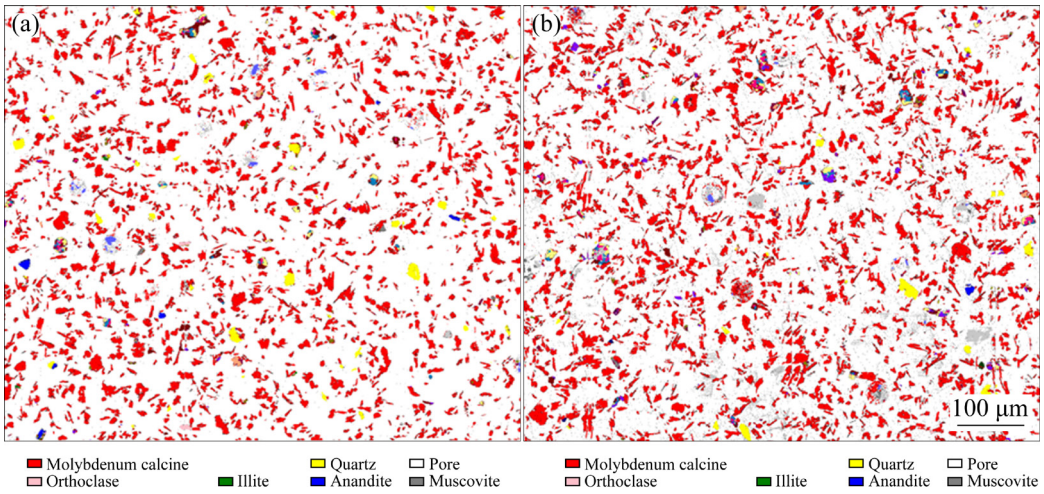

Fig. 9 MLA scan classification images of samples under different cooling methods: (a) Slow cooling; (b) Rapid cooling

Table 8 MLA analysis results of potassium minerals by different cooling methods (wt.%)

Cooling method	Muscovite	Orthoclase	Illite	Anandite	MoO_3
Slow cooling	0.1	0.17	0.02	0.46	90.6
Rapid cooling	0.15	0.05	0.01	0.44	90.73

As shown in Table 8, the content of MoO_3 in molybdenum calcine under two different cooling methods is almost the same. It indicates that the grade of molybdenum calcine will not be reduced by rapid cooling. However, the content of orthoclase under rapid cooling conditions is significantly lower than that of slow cooling. The illite and anandite content under rapid cooling is slightly lower than that under slow cooling, and the muscovite content under rapid cooling is 0.15%, which is 50% higher than 0.1% under slow cooling. Through combining the results in Table 6, it can be seen that the muscovite content in the molybdenum concentrate before roasting is 0.36%. Therefore, it can be inferred that the muscovite has undergone significant transformation during the roasting process.

The main reason is that the temperature of molybdenum calcine can be quickly reduced to below the decomposition temperature of muscovite by means of rapid cooling. It is beneficial to inhibiting the transformation of muscovite into orthoclase, thereby reducing the potassium content in ammonium molybdate.

4 Conclusions

(1) In the water washing and ammonia leaching process, the best kinetic model of potassium release was the first-order reaction model. The maximum equilibrium release of potassium during ammonia leaching was greater than that of water washing, which had a great impact on the quality of ammonium molybdate products.

(2) During the high temperature roasting process, muscovite could be decomposed to form orthoclase, and it would also react with impurity elements to generate anandite. The amount of potassium released by different minerals into the ammonium molybdate solution during the ammonia leaching process is: orthoclase > muscovite > anandite > illite.

(3) The method of rapid cooling could significantly reduce the content of orthoclase in molybdenum calcine. It had a positive effect on reducing the potassium content in ammonium molybdate products.

Acknowledgments

The authors are grateful for the financial support from the Natural Science Foundation of Shaanxi Province, China (No. 2019JLM-34).

References

[1] TANG Jun-li, CAO Wei-cheng, TANG Li-xia, LI Xue-wu, WU Zhou, WU Hong-xu. Review of potassium removal from molybdenum [J]. China Molybdenum Industry, 2017, 41(3): 34−36. (in Chinese)

[2] QIN Jing, LIU De-fu, ZHANG Ying-hui, LAI Chao-bin. Application status and development prospect of rare earth in electrical steels [J]. Journal of Iron and Steel Research, 2018, 30(3): 163−170. (in Chinese)

[3] GAN Min, FAN Xiao-hui, CHEN Xu-ling, WU Cheng-qian, JI Zhi-yun, WANG Song-rong, WANG Guo-jing, QIU Guan-zhou, JIANG Tao. Reaction mechanisms of low-grade molybdenum concentrate during calcification roasting process [J]. Transactions of Nonferrous Metals Society of China, 2016, 26(11): 3015−3023.

[4] TANG Li-xia, LI Xue-wu, LIU Dong-xin. Analysis of soluble change mechanism of potassium minerals during roasting of molybdenum concentrate [J]. China Molybdenum Industry, 2016, 40(5): 42−43,49. (in Chinese)

[5] LI Tong, VIRGINIE M, KHODAKOV A Y. Effect of potassium promotion on the structure and performance of alumina supported carburized molybdenum catalysts for Fischer-Tropsch synthesis [J]. Applied Catalysis A: General, 2017, 542: 154−162.

[6] SHEN Yi-rui, JIANG Ping-ping, WAI P T, GU Qian, ZHANG Wei-jie. Recent progress in application of molybdenum-based catalysts for epoxidation of alkenes [J]. Catalysts, 2019, 9(1): 31.

[7] WANG Lu, ZHANG Guo-hua, WANG Song-Jing, CHOU Kuo-chih. Influences of different components on agglomeration behavior of MoS_2 during oxidation roasting process in air [J]. Metall Mater Trans B, 2016, 47(4): 2421−2432.

[8] MAHMOODI T, MANSOURI M. Structural effects of substitutional impurities on MoO_3 bilayers: A first principles study [J]. Journal of the Korean Physical Society, 2016, 69(9): 1439−1444.

[9] ZHANG Guo-hua, CHANG He-qiang, WANG Lu, CHOU Kuo-chih. Study on reduction of MoS_2 powders with activated carbon to produce Mo_2C under vacuum conditions [J]. Int J Miner Metall Mater, 2018, 25(4): 405−412.

[10] KAN S, BENZEŞIK K, ODABAŞ Ö C, YÜCEL O. Investigation of molybdenite concentrate roasting in chamber and rotary furnaces [J]. Mining, Metallurgy & Exploration, 2021, 38(3): 1597−1608.

[11] SHEKHTER L N, LITZ J E, SHAH N M, MCHUGH L F. Thermodynamic modelling of molybdenite roasting in a multiple-hearth furnace [J]. JOM, 2021, 73(3): 873−880.

[12] FAN Jian-jun, YANG Yan, LI Hui, LI Li. Experimental study on extraction and recovery of molybdenum from molybdenum concentrate acid pickling wastewater [J]. China Molybdenum Industry, 2014, 38(2): 7−10. (in Chinese)

[13] JIANG Yong-lin, LIU Bing-guo, LIU Peng, PENG Jin-hui, ZHANG Li-bo. Dielectric properties and oxidation roasting of molybdenite concentrate by using microwave energy at 2.45 GHz frequency[J]. Metall Mater Trans B, 2017, 48(6): 3047−3057.

[14] WU Hong-xu, LI Wei-chang. Study on potassium composition and morphological transfomation factors during roasting and quenching process [J]. China Molybdenum Industry, 2015, 39(4): 36−39. (in Chinese)

[15] ZHANG Meng-ping, LIU Chen-hui, ZHU Xiong-jin, XIONG Hua-bin, ZHANG Li-bo, GAO Ji-yun, LIU Man-hong. Preparation of ammonium molybdate by oxidation roasting of molybdenum concentrate: A comparison of microwave roasting and conventional roasting [J]. Chemical Engineering and Processing: Process Intensification, 2021: 108550.

[16] TANG Jun-li, CUI Yu-qing, CAO Wei-cheng, TANG Li-xia, LI Xue-wu, WU Zhou, WU Hong-xu. Source apportionment of potassium from ammonium molybdate [J]. China Molybdenum Industry, 2017, 41(6): 36−38. (in Chinese)

[17] WANG Lu, ZHANG Guo-hua, DANG Jie, CHOU Kuo-chih. Oxidation roasting of molybdenite concentrate [J]. Transactions of Nonferrous Metals Society of China, 2015, 25(12): 4167−4174.

[18] XIE Keng, WANG Hai-bei, WANG Sheng-dong. Direct leaching of molybdenum and lead from lean wulfenite raw ore [J]. Transactions of Nonferrous Metals Society of China, 2019, 29(12): 2638−2645.

[19] LI Xiao-bin, WU Tao, ZHOU Qiu-sheng, QI Tian-gui, PENG Zhi-hong, LIU Gui-hua. Kinetics of oxidation roasting of molybdenite with different particle sizes [J]. Transactions of

Nonferrous Metals Society of China, 2021, 31: 842−852.
[20] FAN Xiao-hui, DENG Qiong, GAN Min, Chen Xu-ling. Roasting oxidation behaviors of ReS_2 and MoS_2 in powdery rhenium-bearing, low-grade molybdenum concentrate [J]. Transactions of Nonferrous Metals Society of China, 2019, 29(4): 840−848.
[21] ARACENA A, SANINO A, JEREZ O. Dissolution kinetics of molybdite in KOH media at different temperatures [J]. Transactions of Nonferrous Metals Society of China, 2018, 28(1): 177−185.
[22] LODI L A, RODRIGO K, CAUE R, FARINAS C S. A green K-fertilizer using mechanical activation to improve the solubilization of a low-reactivity potassium mineral by *Aspergillus niger* [J]. Bioresource Technology Reports, 2021: 100711.
[23] ZHANG Zi-chen, XIE-He. Study on silicate bacteria strains to release potassium from two kinds of insoluble potassium-bearing mineral [J]. Guangdong Agricultural Sciences, 2013, 40(4): 43−46. (in Chinese)
[24] WANG Lu, ZHANG Guo-hua, CHOU Kuo-chih. Study on oxidation mechanism and kinetics of MoO_2 to MoO_3 in air atmosphere [J]. International Journal of Refractory Metals and Hard Materials, 2016, 57: 115−124.
[25] LAAKOS K, MIDDLETON M, HEINIG T, BÄRS R, LINTINEN P. Assessing the ability to combine hyperspectral imaging (HSI) data with Mineral Liberation Analyzer (MLA) data to characterize phosphate rocks [J]. International Journal of Applied Earth Observation and Geoinformation, 2018, 69: 1−12.
[26] XU Cai-li, ZHONG Cheng-bin, LYU Ren-liang, RUAN Yao-yang, ZHANG Zhen-yue, CHI Ru-an. Process mineralogy of Weishan rare earth ore by MLA [J]. Journal of Rare Earths, 2019, 37(3): 334−338.
[27] CAMALAN M, ÇAVUR M. Development of a supervised classification method to construct 2D mineral mapson backscattered electron images [J]. Turkish Journal of Electrical Engineering and Computer Sciences, 2020, 28(2): 1030−1043.

钼精矿处理流程中杂质钾的释放机理

刘起航[1,2]，胡 蕖[1]，王 帝[1]，杨双平[1]，何 凯[2]

1. 西安建筑科技大学 冶金工程学院，西安 710055；
2. 金堆城钼业股份有限公司 技术中心，西安 710077

摘 要：通过动力学分析和 SEM−EDS、MLA、ICP 等分析技术研究钼精矿处理过程中钾释放的动力学特征和机理。结果表明，钼焙砂在水洗和氨浸过程中钾释放的最佳动力学模型均为一级动力学模型，且钾在钼精矿中主要以可溶性钾离子和 4 种含钾矿物的形式存在。在钼精矿的焙烧过程中，一部分云母分解生成正长石，而另一部分云母则与杂质金属元素结合后形成钡铁云母。此外，快速冷却可有效抑制钼焙砂中云母向正长石的分解转化。研究结果可为降低钼酸铵产品中的钾含量提供依据。

关键词：钼精矿；除钾；焙烧；含钾矿物；钼酸铵

(Edited by Xiang-qun LI)